

Observational benchmarks inform representation of soil organic carbon dynamics in land surface models

Kamal Nyaupane¹, Umakant Mishra^{2*}, Feng Tao³, Kyongmin Yeo⁴, William J. Riley⁵, Forrest M. Hoffman⁶ and Sagar Gautam²

¹Environmental science and Engineering Program, The University of Texas at El Paso, El Paso, TX 79968, United States.

² Biomaterials & Biomanufacturing, Sandia National Laboratories, Livermore, CA, 94550, United States.

³Department of Ecology & Evolutionary Biology, Cornell University, Ithaca, NY, 14850, United States

⁴IBM Thomas J. Watson Research Center, Yorktown Heights, NY, 10562, United States.

⁵Earth & Environmental Sciences, Lawrence Berkeley National Laboratory, Berkeley, CA, 94720, United States.

⁶Climate Change Institute, Oak Ridge National Laboratory, Oak Ridge, TN, 37830, United States.

*Corresponding author Email: umishra@sandia.gov

1 **Abstract**

2 Representing soil organic carbon (SOC) dynamics in Earth system models (ESMs) is a key
3 source of uncertainty in predicting carbon climate feedbacks. Machine learning models can help
4 in the identification of dominant environmental controllers and establishing their functional
5 relationships with SOC stocks. The resulting knowledge can be integrated in ESMs to
6 reduce uncertainty and better predict SOC dynamics over space and time. In this study, we used
7 a large number of SOC field observations ($n = 54,000$), geospatial datasets of environmental
8 factors ($n = 46$), and two machine learning approaches, namely (Random Forest (RF) and
9 Generalized Additive Modeling (GAM)) to: (1) identify dominant environmental controllers of
10 global and biome-specific SOC stocks, (2) derive functional relationships between
11 environmental controllers and SOC stocks, and (3) compare the identified environmental
12 controllers and predictive relationships with those in Coupled Model Intercomparison Project
13 phase six (CMIP6) models. Our results showed that diurnal temperature, drought index, cation
14 exchange capacity, and precipitation were important ~~observed~~ environmental ~~predictors~~ controllers
15 of global SOC stocks. While the RF model identified 14 environmental factors that describes
16 climatic, vegetation and edaphic conditions being important predictors of global SOC stocks
17 ~~predictions of global scale SOC stocks were relatively accurate~~ ($R^2 = 0.61$, $RMSE = 0.46 \text{ kg m}^{-2}$),
18 current ESMs over simplified relationships between the environmental factors and SOC,
19 with. In contrast, precipitation, temperature, and net primary productivity explaining >96% of
20 the variability in ESM-modeled SOC stocks ~~variability~~. Further, our study revealed notable
21 disparities in the ~~We also found very different~~ functional relationships between environmental
22 factors and SOC stocks ~~simulated by ESMs compared to observations~~ ~~in observations and ESMs~~.
23 To enhance SOC representation ~~predictions~~ in ESMs, it is imperative to incorporate ~~may be~~

24 ~~improved significantly by including~~ additional environmental controls ~~such as (e.g.,~~ cation
25 exchange capacity, ~~) and re~~finepresenting the functional relationships ~~to align more closely of~~
26 ~~environmental controllers consistent~~ with observations.

27

28 **Keywords:** Environmental controllers, Earth system models, soil organic carbon, net primary
29 productivity, machine learning, model benchmarking

30

31 **1. Introduction**

32 Soil is the largest actively cycling carbon pool in terrestrial ecosystems and stores almost twice
33 the amount of carbon as in the current atmosphere (Lal, 2016). Even Aa small change in soil
34 carbon stocks can lead to large changes in the atmospheric CO₂ concentration, influencing
35 the and future climate change trajectories. Additionally, Ssoils also play a crucial role in
36 capturesequestering atmospheric CO₂ through the storage of as soil organic carbon (SOC) (Hinge et
37 al., 2018). Therefore us, the sequestration, protection, and sustainable management of SOC stocks
38 can be a promising climate mitigation strategy (Lal, 2020). The Accurate representation of
39 global SOC storage and its environmental controllers is are essential for predicting realistic SOC
40 changes ~~of SOC~~ under different land use and climate change scenarios. However Yet, there is
41 currently no consensus ~~exists~~ among current Earth system models (ESMs) in representing the
42 spatial distributions of global SOC storage and its fate under future climate change scenarios
43 (Friedlingstein et al., 2014.; Arora et al., 2020).

44 Multiple environmental variables, including climatic and topographic factors, land use history,
45 and edaphic properties, have been identified as possible controllers of SOC storage (Georgiou et
46 al., 2021; Mishra et al., 2022). Current ESMs, however, use the effects of only a limited number

47 of environmental factors in representing SOC storage and dynamics. A recent study that
48 compared SOC stocks from multiple ESMs against observations indicated a large knowledge gap
49 in both ESMs and observations (Georgiou et al., 2021). Therefore, it is important to compare
50 ESM simulations against global SOC observational datasets to evaluate model performance and
51 identify key environmental controllers of global SOC storage.

52 Benchmarking ESM simulations with observed data is a common approach for model evaluation
53 (Luo et al., 2012; ~~Todd Brown et al., 2013~~; Collier et al., 2018). Through comparing model
54 simulations with observations, model strengths, deficiencies, and needed improvements can be
55 identified. The resulting understanding from SOC benchmarking could lead to new ESM land
56 model structures (by identifying key processes) and new parameterizations (by quantifying key
57 relationships between SOC and environmental variables). Thus, benchmarking analysis of ESMs
58 is an effective tool to reduce uncertainties in predicting SOC dynamics and can provide more
59 realistic information for managing SOC under changing climate conditions (Lauer et al., 2017).
60 Currently ESMs predict SOC stocks primarily with model representations that depend on soil
61 temperature, moisture, and belowground net primary production (Todd-Brown et al., 2013).
62 ESMs capture the positive correlation between NPP and precipitation, resulting in high SOC
63 stocks for areas with high NPP in moist regions (Sun et al., 2016). Higher temperature increases
64 soil respiration, which, in the short-term, reduces SOC storage. In the longer-term, increased soil
65 respiration can release nutrients, leading to increased plant growth, belowground carbon inputs,
66 and thereby SOC stocks; the balance of these factors can take centuries to manifest (Mekonnen
67 et al., 2022). Soil respiration temperature sensitivity is often defined based on Q_{10} or Arrhenius
68 equations in ESMs (Wynn et al., 2006), although low- and high-temperature modifications to
69 these relationships are likely needed (Jiang et al., 2013; Azizi-Rad et al., 2022).

70 Among environmental factors, soil moisture plays a crucial role in plant growth, microbial
71 activity, carbon inputs, litter and SOC decomposition. Global soil carbon stocks correlate with
72 mean annual precipitation, emphasizing the significance of water availability in SOC dynamics.
73 The relationship between soil moisture and microbial activity follows a curve, reaching a
74 maximum at optimal moisture content. Variations in soil moisture can either hinder or enhance
75 microbial activity, impacting SOC decomposition rates and carbon cycling (Moyano et al., 2013;
76 Wieder et al., 2018; Davidson et al., 2012; Moyano et al., 2018). This non-linear soil moisture
77 function is crucial for predicting SOC turnover, though its specific form varies among models
78 (Sierra et al., 2015). Diverse measures of soil moisture are vital for comprehending water
79 availability across different scales, serving as indicators for soil-water relationships and
80 ecosystem functioning. Previous studies suggest various functional forms, such as linear,
81 quadratic, or asymptotic, to capture the impact of moisture on soil microbial activity, with
82 relative water saturation being a reliable predictor across diverse soil types (Moyano et al.,
83 2013). The temperature function in soil carbon models represents the sensitivity of SOC
84 decomposition to temperature and the availability of soluble substrates that drive carbon
85 substrate decomposition (Davidson et al., 2012). Based on the Q10 equation, a 10°C temperature
86 increase roughly doubles the rate of soil respiration, reflecting increased microbial activity,
87 leading to increased organic matter decomposition and higher CO₂ emissions from the soil.
88 Recent research emphasizes the variability in temperature sensitivity to SOC decomposition is
89 linked to microbial community composition. A comprehensive understanding of the temperature
90 function requires accounting for microbial community dynamics in soil carbon models. This
91 consideration is crucial due to the multifaceted interaction with temperature, involving
92 accelerated microbial activity and faster O₂ depletion, influencing soil oxygen dynamics. The

93 empirical relationship between soil respiration and temperature, represented in the Q10
94 relationship remains essential for predicting the impact of temperature change on soil carbon
95 dynamics and understanding its global implications for carbon cycling (Lloyd and Taylor, 1994).

96 In a previous U.S. continental-scale study, we derived empirical non-linear relationships between
97 SOC and environmental factors that produced comparable prediction accuracy to a random forest
98 (RF) machine learning approach (Mishra et al., 2022). We apply a similar approach in this study
99 in both global field observations and ESMs to (1) identify key observed environmental controllers
100 of, and functional relationships with, global SOC stocks and (2) evaluate ESMs with these
101 observational benchmarks. Simulated SOC stocks from three CMIP6 ESMs (i.e., Community
102 Earth System Model (CESM, Hurrell et al., 2013); U.K. Earth System Model (UKESM, Sellar et
103 al., 2019); Beijing Climate Center model (BCC, Xiao-Ge et al., 2019) were benchmarked with
104 over 50,000 SOC profile observations across the globe. We used a machine learning (i.e., random
105 forest) approach with 46 environmental factors to identify the key environmental controllers of
106 SOC stocks at the global scale. We then applied a generalized additive model (GAM) to derive the
107 predictive relationships between these key environmental factors and SOC stocks in observations
108 and ESM simulations. Specific objectives of this study were to: (1) identify
109 dominant environmental controllers of SOC stocks in field observations and CMIP6 ESM
110 simulations, (2) derive observed and ESM-modeled functional relationships between
111 environmental factors and SOC stocks, and (3) analyze these functional relationships to inform
112 needed improvements in ESM representations of SOC dynamics.

113 **2. Materials and Methods**

114
115 **2.1 Soil organic carbon stock observations**
116

117 We used two datasets of SOC stocks for the upper 30 cm (i.e., 0 – 30 cm) and upper meter of soil
118 (i.e., 0 – 100 cm) topsoil layer (i.e., 0 – 30 cm) and the whole soil profile (i.e., 0 – 100 cm). We
119 note that limiting our analysis to these depth intervals we may not be accounting for the total SOC
120 stocks as in some soils (e.g., peatlands) large SOC stocks can be found to much deeper depths.

121 The World Soil Information Service (WoSIS) compiled SOC profiles across the globe after quality
122 assessment. The 2019 snapshot of the WoSIS dataset contained 111,380 soil profiles with SOC
123 content information (unit: g C g-soil⁻¹) at different soil depths (Batjes et al., 2020). We estimated
124 the SOC stock (g C m⁻²) at different soil layers using:

$$125 \quad SOC\ Stock = SOC\ Content \times \left(1 - \frac{G}{100}\right) \times BD \times D \quad (1)$$

126 where G is the coarse fragment fraction (%); BD is the bulk density of soil (g m⁻³); and D is the
127 soil layer depth (m).

128 When the measured bulk density value was absent from the dataset, we used a pedo-transfer
129 function (Yigini et al., 2018) to estimate the soil bulk density:

$$130 \quad BD = \alpha + \beta \times \exp(-\gamma \times OM) \quad (2)$$

131 Where OM is organic matter, equivalent to SOC×1.724, with SOC content in percent (%); α , β ,
132 and γ are fitting parameters. We found $\alpha = 0.32$, $\beta = 1.30$, and $\gamma = 0.0089$ after fitting WoSIS data
133 to this equation.

134 Another dataset we used in this study was compiled from Mishra et al. (2021). This dataset
135 contained 2,546 soil profiles with SOC stock (g C m⁻³) information from permafrost regions in
136 North America, northern Eurasia, and the Qinghai-Tibet Plateau. In total, we used 113,926 soil
137 profile observations from these two data sources. SOC stocks of different soil layers were then
138 summed to SOC stocks in 0 – 30 cm and 0 – 100 cm depth intervals. Because not all these soil
139 profiles covered the whole 0 – 30 cm or 0 – 100 cm intervals, we used a total of 54,000 soil profiles

140 that included SOC stock information for both depth intervals. The geographical distributions of
141 soil profiles used in this study are shown in Figure 1. Because SOC stock values across the globe
142 were highly skewed, we used a natural logarithm transformation in this study.

143

144 ***2.2 Environmental predictors of SOC stocks***

145

146 The storage and cycling of SOC are controlled by multiple environmental factors. In this study,
147 we used observations of 46 environmental variables, which represented major soil forming factors
148 (McBratney et al., 2003.). Twenty-one of the 46 environmental variables were climatic variables,
149 including annual average temperature, precipitation, evapotranspiration, drought severity index,
150 and statistics for different temporal scales (e.g., during the wettest and driest quarter in a year).
151 Thirteen of the 46 variables described soil properties (e.g., clay content, sand content, silt content,
152 soil texture, pH, and cation exchange capacity). Six variables represented topographic factors (e.g.,
153 elevation and soil depth). Six variables represented land use and land cover types. All the
154 categorical variables were converted to integer variables and the environmental variables were
155 resampled to a common 1 km resolution. The environmental factors, their original spatial
156 resolution, and data sources are provided in the supporting information (Table S1).

157

158 ***2.3 Selection of dominant environmental controllers of SOC stocks***

159

160 We used RF to select dominant environmental predictors of SOC stocks within biomes and at
161 global scale in both observations and ESMs. RF is an ensemble learning method, which is an
162 extension of the classical Classification and Regression Trees (CART). Building a collection of
163 uncorrelated CARTs through bootstrapping the samples and applying the random subspace method
164 at each branch of the trees, RF improves the prediction performance (Breiman, 2001; Wiesmeier
165 et al., 2011; Mishra et al., 2020). RF is well known for its strength in modeling highly nonlinear

166 relationships between the predictors and is robust to overfitting (Chagas et al., 2016). Moreover,
167 RF is not very sensitive to the choice of the hyperparameters, which makes RF one of the most
168 popular off-the-shelf model for many classification and regression problems.
169 In this study, we trained the RF model using SOC content as a response variable and environmental
170 factors as predictors. The model performance was evaluated using ~~the~~ coefficient of determination
171 (R^2) and root mean square error (RMSE). A 10-fold cross-validation was used to compute R^2 and
172 RMSE. Biome-specific analyses were conducted on a subset of the global dataset. For biome
173 classification, we used the IGBP land classes (Loveland and Belward, 1997). The “Random-
174 Forest” package in R was used to train a RF model using all the observed environmental factors in
175 the dataset and to identify dominant environmental controllers of SOC stocks. Prior to fitting into
176 the final model, we performed a potential collinearity test among the environmental variables by
177 calculating pairwise correlations and variance influence factors. Predictors showing a variance
178 influence factor (VIF) value greater than 10 were omitted, leaving 14 uncorrelated environmental
179 predictors of SOC stocks in the observations.

180

181 ***2.4 Generalized additive model***

182

183 Generalized additive model (GAM) is an extension of generalized linear models, which employs
184 spline functions to model nonlinear relationships between predictor and response variables (Arnold
185 et al., 2013). In GAM, the relationship between predictor and response variable can be modeled as
186 (Hastie and Tibshirani, 1987):

$$187 Y = C + \sum_{i=1}^p f_i(X_i) \quad (3)$$

188 Here, Y is the response variable (SOC), C is a constant, X_i are the environmental controller
189 variables, f_i is a spline function for X_i , and p is the total number of environmental controllers. We

190 used the “mgcv” package in R to build nonlinear relationships between environmental factors and
191 SOC stocks using GAMs for both the SOC field observations as well as CMIP6 ESMs simulated
192 SOC data (Arnold et al., 2013). The performance of GAMs was evaluated by using R^2 and RMSE.

193

194 **2.5 Earth system model outputs**

195

196 We downloaded and aggregated the SOC and environmental controller data from three ESMs that
197 participated in CMIP6: Community Earth System Model (Hurrell et al., 2013.), U.K. Earth System
198 Model (Sellar et al., 2019), and Beijing Climate Center model (Xiao-Ge et al., 2019). These ESMs
199 included most of the environmental factors used by CMIP6 ESMs. ESMs did not report depth-
200 dependent soil carbon projections, making direct comparison with depth-dependent SOC
201 observations difficult. The majority of land models used in ESMs were designed to simulate topsoil
202 carbon for topsoil depth; thus, we assumed that the simulated soil carbon is contained within 1 m
203 of soil profile to simplify comparison with observations.

204

205 **3. Results**

206

207 **3.1 Descriptive statistics of SOC observations**

208

209 The average global SOC stock within the 0 - 1 m depth interval was 13.5 kg C m^{-2} , ranging from
210 $0.14 - 435.3 \text{ kg C m}^{-2}$. Our results indicate substantial variability in global scale SOC observations
211 as the standard deviation (18.2 kg C m^{-2}) was greater than the average SOC stocks. Summary
212 statistics of SOC stocks at global scale and within different biomes is presented in Table 1. Boreal
213 forests and Temperate forests exhibited higher SOC stocks compared to other biomes, while tundra
214 and tropical and subtropical broadleaf forests displayed lower and relatively similar average SOC
215 stocks. Tundra and tropical and subtropical grasslands and savannas exhibited similar and lower
216 standard deviations in SOC stock values. The standard deviation showed a similar spread in SOC

217 ~~stock values in croplands (n=21820), savannas (n=9807) and grasslands (n=5938).~~
218 ~~However Conversely, in boreal forests (n=12164) and shrublands (n=3769), showed higher the~~
219 ~~standard deviation, indicating a broader range in SOC stock values, was higher indicating a large~~
220 ~~range in SOC stock values.~~ Distributions of total SOC stocks in different biomes are presented in
221 ~~Figure 2. Across different biomes, forests contain the largest organic carbon content globally, with~~
222 ~~a mean value of 15.9 kg C m⁻² and standard deviation 20.7 kg C m⁻².~~

223

224
225 **3.2 Dominant environmental controllers of SOC stocks in observations and ESMs**
226

227 At the global scale, we found that diurnal temperature, drought severity index, annual
228 temperature, and cation exchange capacity are the dominant environmental controllers of SOC
229 stocks in observations (Figure 3). By including all the environmental controllers, the RF model
230 explained 61% of observed global spatial SOC variation. R^2 ranged from 48% in boreal
231 forestssavannas to 62% in croplands (Table 2) and the importance of key environmental
232 controllers varied between biomes (Figure 4). In croplands, precipitation, drought, diurnal
233 temperature, and cation exchange capacity were identified as the dominant controllers of SOC
234 stocks. In grasslands, annual temperature, cation exchange capacity, and sand content were the
235 dominant controllers. In forests, cation exchange capacity, precipitation, and temperature were
236 dominant controllers. In shrublands, annual temperature, soil pH, and cation exchange capacity
237 were the most important controllers. In savannas, soil related variables, temperature, and
238 precipitation were the most important controllers. Across all land cover types, we found that
239 cation exchange capacity and seasonal climatic variables were the dominant environmental
240 controllers of SOC stocks.

241 In contrast, the RF model with 8 environmental variable predictors made near-perfect
242 predictions of ESM simulated SOC stocks (average $R^2 = 0.95$, R^2 values for UKESM, CESM,
243 and BCC model were 0.99, 0.89, and 0.98, respectively). In contrast to the results obtained from
244 the observed SOC stocks, the dominant controllers of ESM simulated SOC stocks were annual
245 temperature, net primary productivity (NPP), and annual precipitation (Figure 5). In particular,
246 NPP was by far the most dominant predictor of SOC stocks in the UKESM.

247

248 ***3.2 Predictive relationships between environmental factors and SOC stocks***

249 Dominant environmental controllers of observed SOC stocks identified by the RF model
250 were used in GAM to derive predictive relationships. We retrieved explicit analytical
251 expressions by fitting the splines derived from GAM in the observation dataset. Notwithstanding
252 its role as the sole carbon source to soil, our results did not show NPP as a strong controller on
253 observed SOC stocks (Figure 6a). In contrast with field observations, all ESMs showed
254 significant dependence (exponential increase) of SOC stocks on NPP. Our results also showed
255 that observed SOC stocks increased almost linearly with observed annual precipitation (Figure
256 6b). In contrast, ESMs show different relationships between SOC and precipitation. We found a
257 nonlinearly increasing SOC with precipitation in CESM, an initial sharply increasing and then
258 decreasing relationship in UKESM, and a decreasing relationship in BCC ESM. On the
259 relationship between SOC storage and soil texture and elevation, ESMs do not capture the
260 observed relationships. Our results indicated that observed SOC stocks decreased with clay
261 content in the interval between 0 and 20%, and then increased with clay content above 20%
262 (Figure 6c). Observed SOC stocks increased with silt content up to 55% and then decreased
263 (Figure 6d).

264 SOC stock functional relationships differed between the three ESMs and in many cases
265 differed with the relationships we derived from observations. In terms of the effects of annual
266 temperature on modeled SOC storage, we found that SOC stocks decreased with annual
267 temperature and were most sensitive to temperature in the range between 0 and 10°C (Figure 6e).
268 However, while the three ESMs captured the general negative relationship between SOC storage
269 and temperature, none of them correctly described the varying sensitivity of SOC in different
270 temperature ranges (especially in extreme temperature ranges $<0^{\circ}\text{C}$ and $>20^{\circ}\text{C}$). In representing
271 the control of elevation on SOC storage, only UKESM showed consistent patterns with
272 observations, where SOC storage remained stable when the elevation was lower than 2000 m and
273 decreased when the elevation was higher than 2000 m (Figure 6f).

274

275 **Discussion**

276 Previous studies have suggested that the spatial variation of SOC is dependent on multiple
277 environmental factors such as climatic and edaphic variables, geography, and vegetation. Here,
278 we found that climatic variables (i.e., temperature and precipitation) are the most important
279 controllers of global SOC stocks, followed by edaphic variables (i.e., cation exchange capacity),
280 topography (i.e., elevation), and vegetation (i.e., NPP). Using boosted regression trees, Luo et al.
281 (2021) studied edaphic and climatic controls on SOC dynamics at different soil depths and found
282 that soil type and climatic variables are the most important variables in explaining the SOC
283 stocks (Luo et al., 2021). In this study, we found that seasonal climatic variables such as diurnal
284 temperature range and precipitation seasonality are among the most important environmental
285 controllers in explaining the spatial variation of SOC stocks. This result indicates the critical role
286 of seasonal and interannual climatic variables in understanding SOC dynamics.

287 The importance of climatic variables on global SOC storage emerges from close links
288 with processes that affect ecosystem productivity and soil microbial processes. Consistent with
289 our findings, Wiesmeier et al. (2014) reported climatic variables (temperature and precipitation)
290 as significant controllers of SOC stocks up to 1 m depth in German soils under oceanic climate
291 ([Wiesmeier et al., 2014](#)). Sreenivas et al. (2014) used RF to predict the SOC variability across
292 semi-arid and humid areas of India in the top 30 cm of soil and found that the top three
293 environmental controllers were land cover, mean temperature of hottest months, and mean
294 annual precipitation ([Sreenivas et al., 2016](#)). In our analysis, the overall relative importance of
295 climatic variables was significantly higher than other variables at the global and biome scales.

296 Soil properties were identified as the second most important controllers of global SOC
297 stocks. Soil properties impact various processes that govern soil carbon dynamics. For example,
298 soil properties impact microbial activity, porosity, and oxygen availability in the soil profile,
299 which directly or indirectly control soil water dynamics, plant growth, and SOC stocks.
300 Consistent with our findings, Luo et al. (2021) reported that sand content, silt content, and soil
301 pH were significant controllers of SOC stocks in all soil depths globally.

302 The Palmer drought severity index, which indicates low soil moisture availability, was a
303 dominant controller of global SOC stocks. [Drought severity and duration play crucial roles in](#)
304 [influencing the extent of soil carbon losses through microbial respiration \(Borken and Matzner,](#)
305 [2009\). A decline in soil CO₂ efflux is observed as precipitation events decrease in both quantity](#)
306 [and frequency \(Harper et al., 2005\). In the initial phases of drought, heightened soil CO₂](#)
307 [emissions occur due to the rapid response of plants and microorganisms to environmental stress](#)
308 [\(Ru et al., 2018\). As drought intensifies, the overall CO₂ emission diminishes due to reduced](#)
309 [root growth and microbial CO₂ efflux caused by increasing soil dryness \(Hasibeder et al., 2015\).](#)

310 Similar to the impact of drought duration, intensification of drought results in a decrease in total
311 CO₂ emission by suppressing soil microbial activity and associated soil CO₂ fluxes (Harper et
312 al., 2005; Hu et al., 2020).

313 ~~Consistent with our findings, Li et al. (2021) reported that soil particle size and soil water~~
314 ~~content were the most influential predictors of SOC variation (Li et al., 2021). Soil drought,~~
315 ~~indicating more negative soil water potential and low soil hydraulic conductivity, can cause tree~~
316 ~~mortality (Anderegg et al., 2012). Climate extremes like droughts can impact the structure,~~
317 ~~composition, and functioning of terrestrial ecosystems and can thereby severely affect the~~
318 ~~regional carbon cycle (Frank et al., 2015).~~

319 Cation exchange capacity is a soil property that indicates the active soil surface to which
320 SOC may be adsorbed, and polyvalent metal cations can play a significant role in SOC
321 stabilization by binding organic compounds to mineral surfaces (O'Brien et al., 2015; Solly et
322 al., 2020). O'Brien et al., (2015) found that exchangeable soil Ca²⁺ is a significant predictor of
323 SOC stocks. This relationship is supported by the mechanism that Ca²⁺ and Mg²⁺ promote clay
324 flocculation and bind organic matter to clay surfaces. Solly et al. (2020) reported that SOC and
325 cation exchange capacity are significantly related in both topsoil and subsoil with strong positive
326 relationship.

327 After climatic factors and cation exchange capacity, topography and vegetation (NPP)
328 were important controllers of observed global SOC stocks. Effects of NPP on observed SOC
329 stocks was found to be small (~6% in 0-100 cm soil depth). Similar to our findings, Luo et al.
330 (2021) reported NPP explaining about 10% of the variation of SOC stocks. NPP delivers the
331 primary inputs of carbon to soil and NPP generally increases with moisture, temperature, and
332 CO₂ up to a certain limit (Todd-Brown et al., 2013). NPP also depends on the availability of soil

333 nutrients. Most ESMs overestimate the increase in SOC pools in response to NPP increases
334 (Todd-Brown et al., 2013). The effects of NPP on SOC also depend on biome type and soil
335 depths (Luo et al., 2021; Georgiou et al., 2021). The contribution of NPP on SOC stocks mostly
336 depends on how much NPP ends up in the soil and how it is translocated to different soil depths.
337 Georgiou et al. (2021) reported a saturating relationship of SOC stocks with increasing NPP in a
338 global observational dataset. However, Chen et al., (2018) reported high SOC stocks with
339 increasing productivity and soil water holding capacity (Chen et al., 2018).

340 The three CMIP6 ESMs we analyzed predicted SOC stocks mostly as a function of
341 temperature, precipitation, and NPP. These ESMs simulated positive correlations between SOC
342 stocks and NPP (Figure 6^a), resulting in high SOC stocks in areas with high NPP in most
343 regions (Shi et al., 2013; Sun et al., 2016). In these ESMs, effects of temperature and
344 precipitation on SOC stocks are driven by soil respiration. Most current ESMs simulate the
345 response of soil respiration to temperature using either a Q₁₀ or Arrhenius equation (Wynn et al.,
346 2006), such that a higher temperature causes more soil respiration, and, all else equal, eventually
347 reduces SOC stocks (Figure 6^b). Our results showed diverse control of precipitation on SOC
348 stocks in different ESMs. Todd-Brown et al. (2013) showed that ESM soil respiration either
349 increases monotonically with precipitation, or first increases to a plateau under optimal
350 precipitation and then decreases with further increasing precipitation. Consistent with those
351 results, the ESMs we analyzed in this study showed different dependence of SOC storage on
352 annual precipitation (Figure 6b).

353 In this study, we found that, while current ESMs consider key environmental controllers
354 such as soil temperature and moisture in regulating SOC storage, they show large inter-model
355 variations in representing the functional relationships between these factors and SOC at the

356 global scale. Meanwhile, none of the three ESMs investigated in this study show agreement with
357 in comparison to the patterns that emerged from observations, ~~ESMs have distinctively different~~
358 ~~emergent relationships between environmental factors and SOC stocks~~. These results
359 ~~could signify potential either result from~~ unrealistic parameterization or missing critical
360 processes in model representation. Moreover, Our results highlight the importance of including
361 other environmental factors in simulating global SOC storage. The observed show that observed
362 global SOC stocks are formed beyond the processes currently considered in ESMs such as
363 ~~controlled not only by~~ temperature, precipitation, and NPP. Effects of other environmental
364 factors, such as drought severity index and cation exchange capacity should also be considered in
365 future representations of SOC dynamics in ESMs. ~~It is also imperative to compare Our results~~
366 showed the critical role of observational data ~~in benchmarking and~~ ESM simulations ~~to~~
367 improve and informing model structures and parameterization. While our findings can not
368 directly be used to develop model parameterizations, they can: (1) point to categories of
369 functional forms for controllers; (2) inform where effort may best apply to improve model
370 functional forms (e.g., to the dominant controllers); and (3) inform modelers of where their
371 model may have very different functional forms for emergent relationships than exist in the
372 observations.

373 We note that though not represented in current generation of ESMs use of ecosystem
374 specific (for example croplands or forests) environmental factors such as presence or absence of
375 certain species (for e.g., earthworms or termites) or indicators of anthropogenic management of
376 land (for e.g., use of fertilizers or conservation agriculture practices) may improve the SOC stock
377 prediction accuracy in observations.

379

380

381

382 **5. Conclusion**

383 Our results document disagreement between environmental controllers of SOC stocks in
384 observations and CMIP6 ESM simulations ~~land models~~. Specifically, while the global SOC
385 observations indicate NPP, annual temperature, and annual precipitation have dominant control
386 ~~in modeled SOC stocks. In contrast,~~ diurnal temperature, drought index, annual temperature,
387 cation exchange capacity, and other soil related variables are critical in the dominant
388 ~~controlling~~ers of observed SOC stocks at the global scale, ESMs overstate the role of NPP,
389 annual temperature, and annual precipitation in simulating SOC stocks. Moreover, . Using field
390 ~~observations and data for environmental factors, machine learning techniques predict about 60%~~
391 ~~of the variability in observed global SOC stocks, while in ESMs, only a few environmental~~
392 ~~factors predict about 95% of the variability in predicted SOC stocks. Comparisons of derived~~
393 functional relationships between key~~the~~ environmental factors and SOC stocks showed huge
394 uncertainty among ESMs and no agreement with those emerged from observations~~in~~
395 ~~observations and ESM models also show diserepancies. Optimizing current model~~
396 ~~parameterizations and developing new model structures that consider more processes in soil~~
397 ~~carbon cycle to better simulate global SOC storage are critical for future ESMs development.~~
398 Our results highlight the importance of benchmarking ESMs with observations to improve the
399 mechanistic understanding of soil carbon cycle at the global scale.
400 ~~These diserepancies indicate the importance of efforts to benchmark ESM land models and to~~
401 ~~improve the mechanistic representations that are affected by the observed dominant~~

402 ~~environmental controllers. Such an effort could decrease disagreements between observed and~~
403 ~~modeled SOC stocks.~~

404

405 **Acknowledgements**

406 This study was supported jointly by the Laboratory Directed Research and Development
407 program of Sandia National Laboratories and the Reducing Uncertainties in Biogeochemical
408 Interactions through Synthesis and Computation Science Focus Area (RUBISCO SFA), which is
409 sponsored by the Regional and Global Model Analysis (RGMA) activity of the Earth
410 Environmental Systems Modeling (EESM) Program in the Earth and Environmental Systems
411 Sciences Division (EESD) of the Office of Biological and Environmental Research (BER) in
412 the US Department of Energy Office of Science. Sandia National Laboratories is a multimission
413 laboratory managed and operated by National Technology and Engineering Solutions of Sandia,
414 LLC, a wholly owned subsidiary of Honeywell International, Inc., for the U.S. Department of
415 Energy's National Nuclear Security Administration under contract DE-NA-0003525. Lawrence
416 Berkeley National Laboratory (LBNL) is managed by the Regents of the University of California
417 for the U.S. Department of Energy under Contract No. DE-AC02-05CH11231. Oak Ridge
418 National Laboratory (ORNL) is managed by UT-Battelle, LLC, for the U.S. Department of
419 Energy under Contract No. DE-AC05-00OR22725.

420 **References**

421
422 Anderegg, W. R. L., Berry, J. A., Smith, D. D., Sperry, J. S., Anderegg, L. D. L., and Field, C.
423 B.: The roles of hydraulic and carbon stress in a widespread climate-induced forest die-off, Proc
424 Natl Acad Sci U S A, 109, 233–237, <https://doi.org/10.1073/PNAS.1107891109>, 2012.
425
426 Arnold, D., Wagner, P., and Baayen, R. B.: Using generalized additive models and random
427 forests to model prosodic prominence in German, isca-speech.org, 2013.
428
429 Arora, V., Katavouta, A., Williams, R., Jones, C. D., Brovkin, V., Friedlingstein, P., Schwinger, J., Bopp, L., Boucher, O., Cadule, P., Chamberlain, M., Christian, J., Delire, C., Fisher, R.,
430 Hajima, T., Ilyina, T., Joetzjer, E., Kawamiya, M., Koven, C., Krasting, J., Law, R., Lawrence, D., Lenton, A., Lindsay, K., Pongratz, J., Raddatz, T., Séférian, R., Tachiiri, K., Tjiputra, J.,
431 Wiltshire, A., Wu, T., and Ziehn, T.: Carbon–concentration and carbon–climate feedbacks in
432 CMIP6 models and their comparison to CMIP5 models, Biogeosciences, 17, 4173–4222,
433 <https://doi.org/10.5194/bg-17-4173-2020>, 2020.
434
435
436
437 Azizi-Rad, M., Guggenberger, G., Ma, Y., and Sierra, C. A.: Sensitivity of soil respiration rate
438 with respect to temperature, moisture and oxygen under freezing and thawing, Soil Biology and
439 Biochemistry, 165, <https://doi.org/10.1016/j.soilbio.2021.108488>, 2022.
440
441 Batjes, N., Ribeiro E., and Oostrum, A.: Standardised soil profile data to support global mapping
442 and modelling (WoSIS snapshot 2019), Earth Syst. Sci. Data, 12, 299–320,
443 <https://doi.org/10.5194/essd-12-299-2020>, 2020.
444
445 Breiman, L.: Random forests, Mach Learn, 45, 5–32, <https://doi.org/10.1023/A:1010933404324>,
446 2001.
447
448 Borken, W., and Matzner, E.: Reappraisal of drying and wetting effects on C and N
449 mineralization and fluxes in soils, Glob. Chang. Biol., 15, 808-824, 10.1111/j.1365-
450 2486.2008.01681.x, 2009.
451
452 Chagas, C. da S., Junior, W de C., Bhering, S. B., and Filho, B. C.: Spatial prediction of soil
453 surface texture in a semiarid region using random forest and multiple linear regressions, Catena,
454 139, 232–240, <https://doi.org/10.1016/j.catena.2016.01.001>, 2016.
455
456 Chen, S., Wang, W., Xu, W., Wang, Y., Wan, H., Chen, D., Tang, Z., Tang, X., Zhou, G., Xie, Z., Zhou, D., Shangguan, Z., Huang, J., He, J. S., Wang, Y., Sheng, J., Tang, L., Li, X., Dong, M., Wu, Y., Wang, Q., Wang, Z., Wu, J., Stuart Chapin, F., and Bai, Y.: Plant diversity enhances
457 productivity and soil carbon storage, Proc Natl Acad Sci U S A, 115, 4027–4032,
458 <https://doi.org/10.1073/PNAS.1700298114>, 2018.
459
460
461 Collier, N., Hoffman, F. M., Lawrence, D. M., Keppel-Aleks, G., Koven, C. D., Riley, W. J.,
462 Mu, M., and Randerson, J. T.: The International Land Model Benchmarking (ILAMB) system:
463

464 design, theory, and implementation, Wiley Online Library, 10, 2731–2754,
465 <https://doi.org/10.1029/2018MS001354>, 2018.

466

467 [Davidson, E.A., Samanta, S., Caramori, S.S., and Savage, K.: The Dual Arrhenius and](#)
468 [Michaelis–Menten kinetics model for decomposition of soil organic matter at hourly to seasonal](#)
469 [time scales. Glob. Change Biol., 18, 371-384, https://doi.org/10.1111/j.1365-2486.2011.02546.x, 2012.](#)

470

471

472 Frank, S., Schmid, E., Havlík, P., Schneider, U.A., Böttcher, H., Balkovič, J. and Obersteiner,
473 M.: The dynamic soil organic carbon mitigation potential of European cropland, Global
474 Environmental Change, 35, 269-278, <https://doi.org/10.1016/j.gloenvcha.2015.08.004>, 2015.

475

476 Friedlingstein, P., Meinshausen, M., Arora, V.K., Jones, C.D., Anav, A., Liddicoat, S.K. and
477 Knutti, R.: Uncertainties in CMIP5 climate projections due to carbon cycle feedbacks, Journal of
478 Climate, 27, 511-526, <https://doi.org/10.1175/JCLI-D-12-00579.1>, 2014.

479

480 Georgiou, K., Malhotra, A., Wieder, W. R., Ennis, J. H., Hartman, M. D., Sulman, B. N., Berhe,
481 A. A., Grandy, A. S., Kyker-Snowman, E., Lajtha, K., Moore, J. A. M., Pierson, D., and Jackson,
482 R. B.: Divergent controls of soil organic carbon between observations and process-based models,
483 Biogeochemistry, 156, 5–17, <https://doi.org/10.1007/S10533-021-00819-2>, 2021.

484

485 [Harper, C.W., Blair, J.M., Fay, P.A., Knapp, A.K., Carlisle, J.D.: Increased rainfall variability](#)
486 [and reduced rainfall amount decreases soil CO₂ flux in a grassland ecosystem, Glob. Chang.](#)
487 [Biol., 11, 322-334, https://doi.org/10.1111/j.1365-2486.2005.00899.x, 2005.](#)

488

489 [Hasibeder, R., Fuchslueger, L., Richter, A., Bahn, M.: Summer drought alters carbon allocation](#)
490 [to roots and root respiration in mountain grassland, New Phytol., 205, 1117-1127,](#)
491 [https://doi.org/10.1111/nph.13146, 2015.](#)

492

493 Hastie, T. and Tibshirani, R.: Generalized additive models: Some applications, J Am Stat Assoc,
494 82, 371–386, <https://doi.org/10.1080/01621459.1987.10478440>, 1987.

495

496 Hinge, G., Surampalli, R. Y., and Goyal, M. K.: Prediction of soil organic carbon stock using
497 digital mapping approach in humid India, Environ Earth Sci, 77, <https://doi.org/10.1007/S12665-018-7374-X>, 2018.

498

499

500 [Hu, Z., Chen, H.Y.H., Yue, C., Gong, X.Y., Shao, J., Zhou, G., Wang, J., Wang, M., Xia, J., Li, Y., Zhou, X., and Michaletz, S.T.: Traits mediate drought effects on wood carbon fluxes, Glob.](#)
501 [Chang. Biol., 26, 3429-3442, https://doi.org/10.1111/GCB.15088.](#)

502

503 Hurrell, J.W., Holland, M.M., Gent, P.R., Ghan, S., Kay, J.E., Kushner, P.J., Lamarque, J.F.,
504 Large, W.G., Lawrence, D., Lindsay, K. and Lipscomb, W.H.: The community earth system
505 model: a framework for collaborative research, Bulletin of the American Meteorological Society,
506 94, 1339-1360, <https://doi.org/10.1175/BAMS-D-12-00121.1>, 2013.

507

508 Jiang, H., Deng, Q., Zhou, G., Hui, D., Zhang, D., Liu, S., Chu, G., and Li, J.: Responses of soil
509 respiration and its temperature/moisture sensitivity to precipitation in three subtropical forests in
510 southern China, *Biogeosciences*, 10, 3963–3982, <https://doi.org/10.5194/bg-10-3963-2013>, 2013.
511

512 Lal, R.: Soil health and carbon management, *Food Energy Secur*, 5, 212–222,
513 <https://doi.org/10.1002/fes3.96>, 2016.
514

515 Lal, R.: Managing soils for negative feedback to climate change and positive impact on food and
516 nutritional security, *Soil Sci Plant Nutr*, 66, 1–9,
517 <https://doi.org/10.1080/00380768.2020.1718548>, 2020.
518

519 Lauer, A., Eyring, V., Righi, M., Buchwitz, M., Defourny, P., Evaldsson, M., Friedlingstein, P.,
520 de Jeu, R., de Leeuw, G., Loew, A. and Merchant, C.J.: Benchmarking CMIP5 models with a
521 subset of ESA CCI Phase 2 data using the ESMValTool, *Remote Sensing of Environment*, 203,
522 9–39, <https://doi.org/10.1016/j.rse.2017.01.007>, 2017.
523

524 Lloyd, J., and Taylor, J. A.: On the temperature dependence of soil respiration. *Funct. Ecol.*, 8,
525 315–323, <https://doi.org/10.2307/2389824>, 1994.
526

527 Li, S., Liu, Y., Lyu, S., Wang, S., Pan, Y., and Qin, Y.: Change in soil organic carbon and its
528 climate drivers over the Tibetan Plateau in CMIP5 earth system models, *Theor Appl Climatol*,
529 145, 187–196, <https://doi.org/10.1007/S00704-021-03631-Y>, 2021.
530

531 Loveland, T. R. and Belward, A. S.: The igbp-dis global 1km land cover data set, discover: First
532 results, *Int J Remote Sens*, 18, 3289–3295, <https://doi.org/10.1080/014311697217099>, 1997.
533

534 Luo, Y. Q., Randerson, J., Abramowitz, G., Bacour, C., Blyth, E., Carvalhais, N., Ciais, P.,
535 Dalmonech, D., Fisher, J., Fisher, R., Friedlingstein, P., Hibbard, K., Hoffman, F., Huntzinger,
536 D., Jones, C. D., Koven, C., Lawrence, D., Li, D. J., Mahecha, M., Niu, S. L., Norby, R., Piao, S.
537 L., Qi, X., Peylin, P., Prentice, I. C., Riley, W., Reichstein, M., Schwalm, C., Wang, Y. P., Xia,
538 J. Y., Zaehle, S., and Zhou, X. H.: A framework for benchmarking land models,
539 [bg.copernicus.org](https://doi.org/10.5194/bgd-9-1899-2012), 9, 1899–1944, <https://doi.org/10.5194/bgd-9-1899-2012>, 2012.
540

541 Luo, Z., Viscarra-Rossel, R.A. and Qian, T.: Similar importance of edaphic and climatic factors
542 for controlling soil organic carbon stocks of the world, *Biogeosciences*, 18, 2063–2073.,
543 <https://doi.org/10.5194/bg-18-2063-2021>, 2021.
544

545 McBratney, A.B., Santos, M.M. and Minasny, B.: On digital soil mapping, *Geoderma*, 117, 3–52,
546 [https://doi.org/10.1016/S0016-7061\(03\)00223-4](https://doi.org/10.1016/S0016-7061(03)00223-4), 2003.
547

548 Mekonnen, Z., Riley, W., ... J. R.-E., and 2022, undefined: Wildfire exacerbates high-latitude
549 soil carbon losses from climate warming, *iopscience.iop.org*, <https://doi.org/10.1088/1748-9326/ac8be6>, 2022.
550

551 Mishra, U., Gautam, S., Riley, W. J., and Hoffman, F. M.: Ensemble Machine Learning
552 Approach Improves Predicted Spatial Variation of Surface Soil Organic Carbon Stocks in Data-
553

554 Limited Northern Circumpolar Region, Front Big Data, 3,
555 <https://doi.org/10.3389/FDATA.2020.528441/FULL>, 2020.

556

557 Mishra, U., Yeo, K., Adhikari, K., Riley, W. J., Hoffman, F. M., Hudson, C., and Gautam, S.:
558 Empirical relationships between environmental factors and soil organic carbon produce
559 comparable prediction accuracy to machine learning, Wiley Online Library, 86, 1611–1624,
560 <https://doi.org/10.1002/saj2.20453>, 2022.

561

562 [Moyano, F. E., Manzoni, S., and Chenu, C.: Responses of soil heterotrophic respiration to](#)
563 [moisture availability: An exploration of processes and models, Soil Biology and](#)
564 [Biochemistry, 59, 72- 85, https://doi.org/10.1016/j.soilbio.2013.01.002, 2013.](#)

565

566 [Moyano, F. E., Vasilyeva, N., and Menichetti, L.: Diffusion limitations and Michaelis–Menten](#)
567 [kinetics as drivers of combined temperature and moisture effects on carbon fluxes of mineral](#)
568 [soils, Biogeosciences, 15, 5031–5045, https://doi.org/10.5194/bg-15-5031-2018, 2018.](#)

569

570 O'Brien, S.L., Jastrow, J.D., Grimley, D.A. and Gonzalez-Meler, M.A.: Edaphic controls on soil
571 organic carbon stocks in restored grasslands, Geoderma, 251, 117-123,
572 <https://doi.org/10.1016/j.geoderma.2015.03.023>, 2015.

573

574 [Ru, J.Y., Zhou, Y.Q., Hui, D.F., Zheng, M.M., and Wan, S.Q.: Shifts of growing-season](#)
575 [precipitation peaks decrease soil respiration in a semiarid grassland, Glob. Chang. Biol., 24,](#)
576 [1001-1011, https://doi.org/10.1111/gcb.13941, 2018.](#)

577

578 Sellar, A. A., Jones, C. G., Mulcahy, J. P., Tang, Y., Yool, A., Wiltshire, A., O'Connor, F. M.,
579 Stringer, M., Hill, R., Palmieri, J., Woodward, S., de Mora, L., Kuhlbrodt, T., Rumbold, S. T.,
580 Kelley, D. I., Ellis, R., Johnson, C. E., Walton, J., Abraham, N. L., Andrews, M. B., Andrews,
581 T., Archibald, A. T., Berthou, S., Burke, E., Blockley, E., Carslaw, K., Dalvi, M., Edwards, J.,
582 Folberth, G. A., Gedney, N., Griffiths, P. T., Harper, A. B., Hendry, M. A., Hewitt, A. J.,
583 Johnson, B., Jones, A., Jones, C. D., Keeble, J., Liddicoat, S., Morgenstern, O., Parker, R. J.,
584 Predoi, V., Robertson, E., Siahaan, A., Smith, R. S., Swaminathan, R., Woodhouse, M. T., Zeng,
585 G., and Zerroukat, M.: UKESM1: Description and Evaluation of the U.K. Earth System Model, J
586 Adv Model Earth Syst, 11, 4513–4558, <https://doi.org/10.1029/2019MS001739>, 2019.

587

588 Shi, X., Mao, J., Thornton, P.E. and Huang, M.: Spatiotemporal patterns of evapotranspiration in
589 response to multiple environmental factors simulated by the Community Land Model,
590 Environmental Research Letters, 8, 024012, <https://doi.org/10.1088/1748-9326/8/2/024012>,
591 2013.

592

593 [Sierra, C. A., Trumbore, S. E., Davidson, E. A., Vicca, S., and Janssens, I.: Sensitivity of](#)
594 [decomposition rates of soil organic matter with respect to simultaneous changes in temperature](#)
595 [and moisture. Journal of Advances in Modeling Earth Systems, 7, 335-356,](#)
596 [https://doi.org/10.1002/2014MS000358, 2015.](#)

597

598 Solly, E. F., Weber, V., Zimmermann, S., Walthert, L., Hagedorn, F., and Schmidt, M. W. I.: A
599 Critical Evaluation of the Relationship Between the Effective Cation Exchange Capacity and

600 Soil Organic Carbon Content in Swiss Forest Soils, *Frontiers in Forests and Global Change*, 3,
601 <https://doi.org/10.3389/FFGC.2020.00098/FULL>, 2020.
602

603 Sreenivas, K., Sujatha, G., Sudhir, K., Kiran, D. V., Fyzee, M. A., Ravisankar, T., & Dadhwal,
604 V. K.: Spatial assessment of soil organic carbon density through random forests based
605 imputation. *Journal of the Indian Society of Remote Sensing*, 42(3), 577-587, [10.1007/s12524-013-0332-x](https://doi.org/10.1007/s12524-013-0332-x), 2014.

607 ~~Sreenivas, K., Dadhwal, V.K., Kumar, S., Harsha, G.S., Mitran, T., Sujatha, G., Suresh, G.J.R.,~~
608 ~~Fyzee, M.A. and Ravisankar, T.: Digital mapping of soil organic and inorganic carbon status in~~
609 ~~India, *Geoderma*, 269, 160-173, https://doi.org/10.1016/j.geoderma.2016.02.002, 2016.~~

610

611 Sun, Y., Piao, S., Huang, M., Ciais, P., Zeng, Z., Cheng, L., Li, X., Zhang, X., Mao, J., Peng, S.,
612 Poulter, B., Shi, X., Wang, X., Wang, Y. P., and Zeng, H.: Global patterns and climate drivers of
613 water-use efficiency in terrestrial ecosystems deduced from satellite-based datasets and carbon
614 cycle models, *Global Ecology and Biogeography*, 25, 311–323,
615 <https://doi.org/10.1111/GEB.12411>, 2016.

616

617 Todd-Brown, K. E. O., Randerson, J. T., Post, W. M., Hoffman, F. M., Tarnocai, C., Schuur, E.
618 A. G., and Allison, S. D.: Causes of variation in soil carbon simulations from CMIP5 Earth
619 system models and comparison with observations, *Biogeosciences*, 10, 1717–1736,
620 <https://doi.org/10.5194/BG-10-1717-2013>, 2013.

621

622 Wieder, W.R., Hartman, M.D., Sulman, B.N., Wang, Y.-P., Kover, C.D., and Bonan, G.B.:
623 Carbon cycle confidence and uncertainty: Exploring variation among soil biogeochemical
624 models, *Global Change Biology*, 24, 1563–1579, https://doi.org/10.1111/gcb.13979, 2018.

625

626 Wiesmeier, M., Barthold, F., Blank, B., and Kögel-Knabner, I.: Digital mapping of soil organic
627 matter stocks using Random Forest modeling in a semi-arid steppe ecosystem, *Plant Soil*, 340,
628 7–24, <https://doi.org/10.1007/S11104-010-0425-Z>, 2011.

629

630 Wiesmeier, M., Barthold, F., Spörlein, P., Geuß, U., Hangen, E., Reischl, A., Schilling, B.,
631 Angst, G., von Lützow, M. and Kögel-Knabner, I.: Estimation of total organic carbon storage
632 and its driving factors in soils of Bavaria (southeast Germany), *Geoderma Regional*, 1, 67-78,
633 <https://doi.org/10.1016/j.geodrs.2014.09.001>, 2014.

634

635 Wynn, J. G., Bird, M. I., Vellen, L., Grand-Clement, E., Carter, J., and Berry, S. L.: Continental-
636 scale measurement of the soil organic carbon pool with climatic, edaphic, and biotic controls,
637 Wiley Online Library, 20, <https://doi.org/10.1029/2005GB002576>, 2006.

638

639 Xiao-Ge, X.I.N., Tong-Wen, W.U., Jie ZHANG, F.Z., Wei-Ping, L.I., Yan-Wu ZHANG,
640 Y.X.L., Yong-Jie, F.A.N.G., Wei-Hua, J.I.E., Li ZHANG, M.D., Xue-Li, S.H.I., Jiang-Long, L.I.
641 and Min, C.H.U.: Introduction of BCC models and its participation in CMIP6, *Advances in*
642 *Climate Change Research*, 15, 533, <https://doi.org/10.12006/j.issn.1673-1719.2019.039>, 2019.

643

644 Yigini, Y., Olmedo, G., Reiter, S., Baritz, R., and Viatkin, K.: Soil organic carbon mapping:
645 cookbook, 2018.
646

Figures and Tables

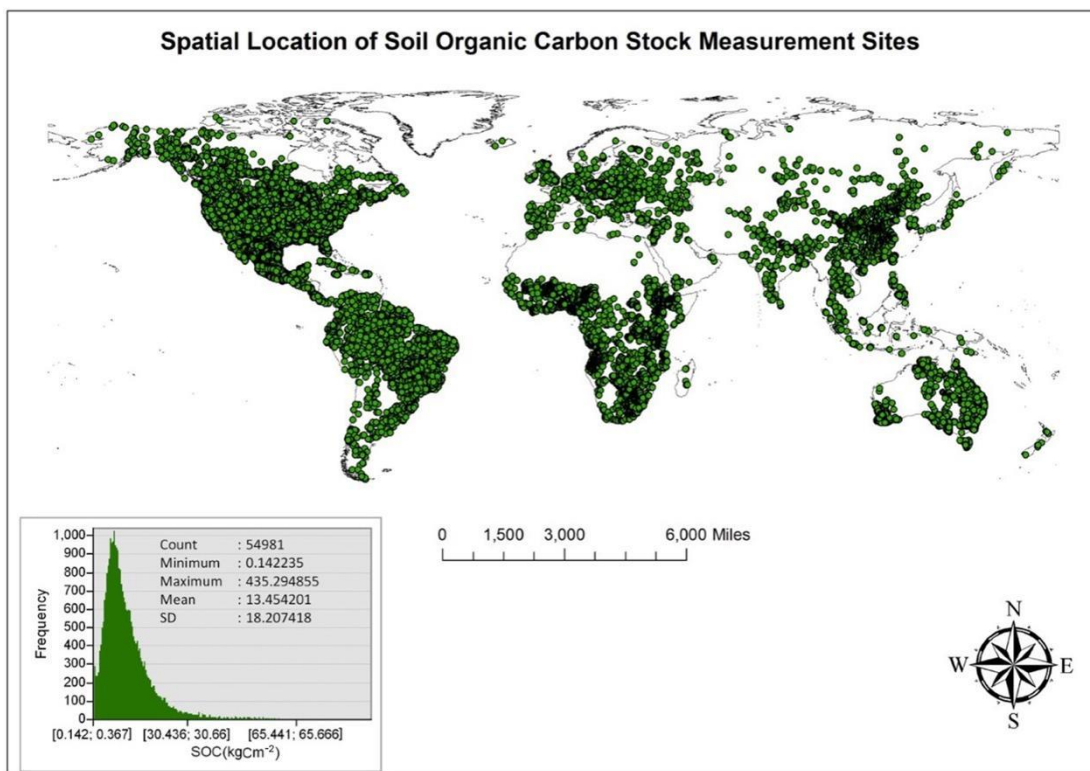


Figure 1. Spatial and statistical distributions of 54,000 soil organic carbon profiles used in this study.

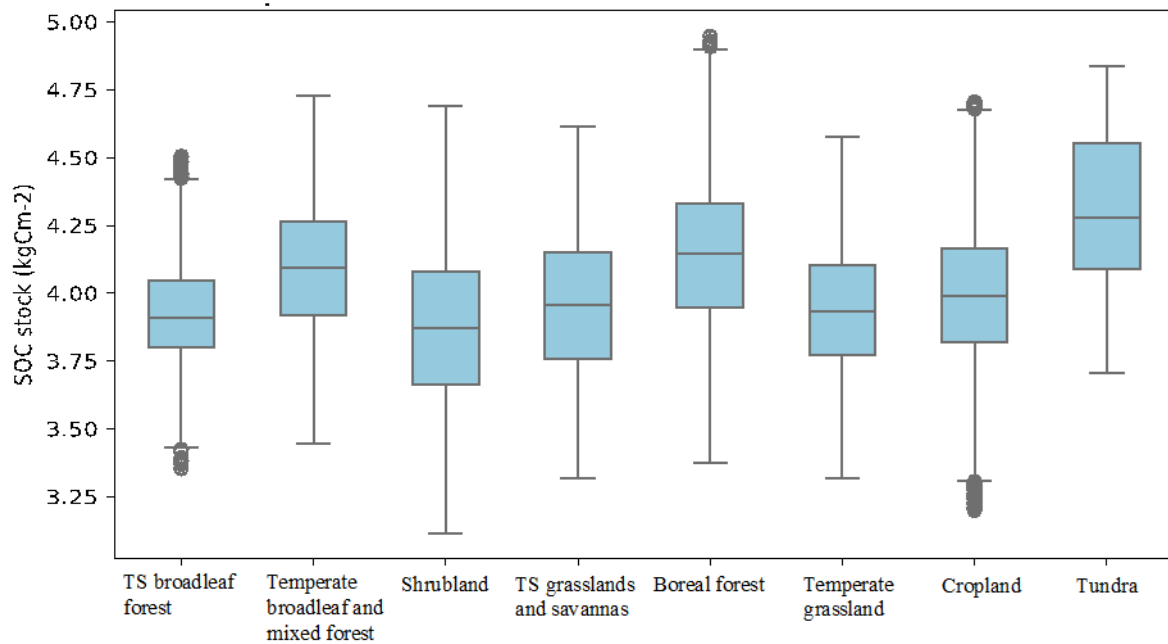


Figure 2: Boxplot of soil organic carbon (SOC) stock for each biome analyzed in this study. The horizontal line in the middle of the boxes is the median while their lower and upper limits correspond to the first and third quartiles. TS is tropical/subtropical.

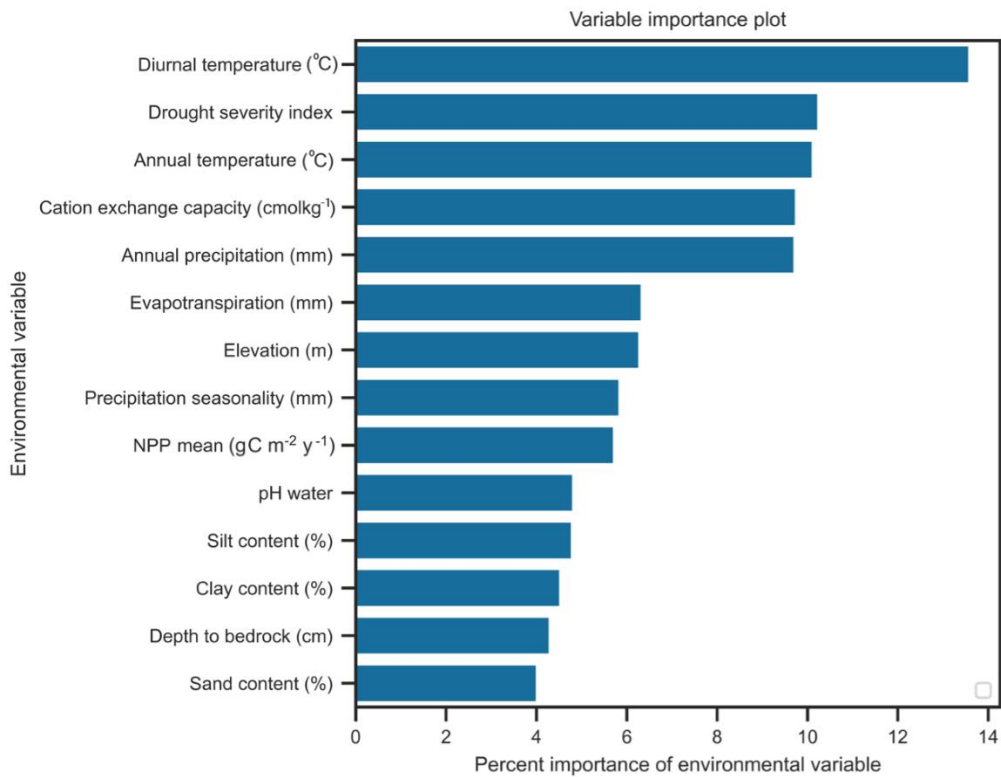


Figure 3: Importance of different environmental factors to predict the global soil organic carbon stocks in observations.

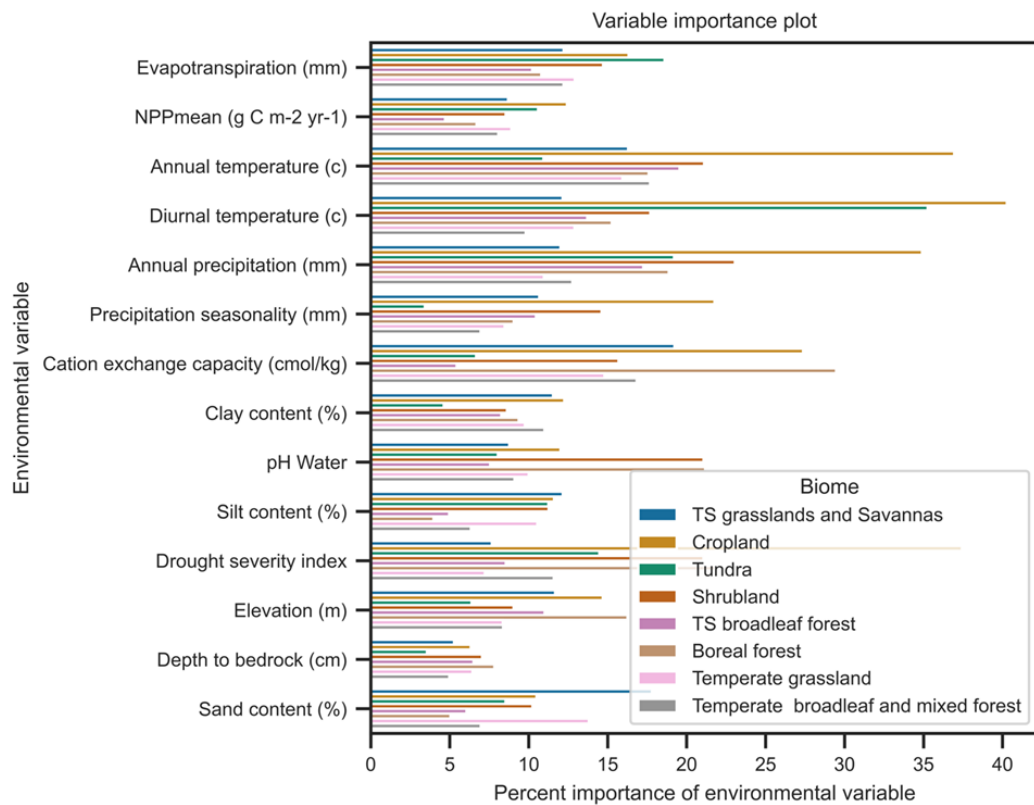


Figure 4: Strengths and importance of environmental ~~facto~~ controllers in predicting of observed SOC stocks within different biomes.

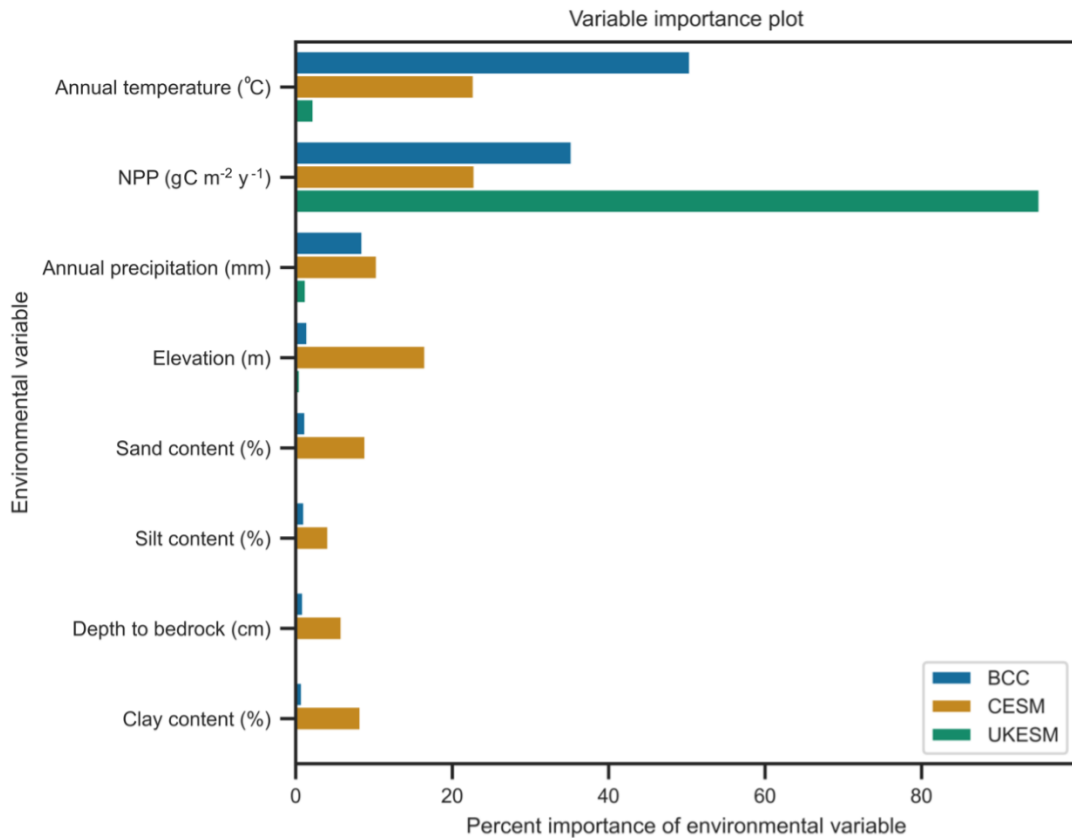


Figure 5: Importance of different environmental factors in predicting ~~on~~ global soil organic carbon stocks in three CMIP6 earth system models.

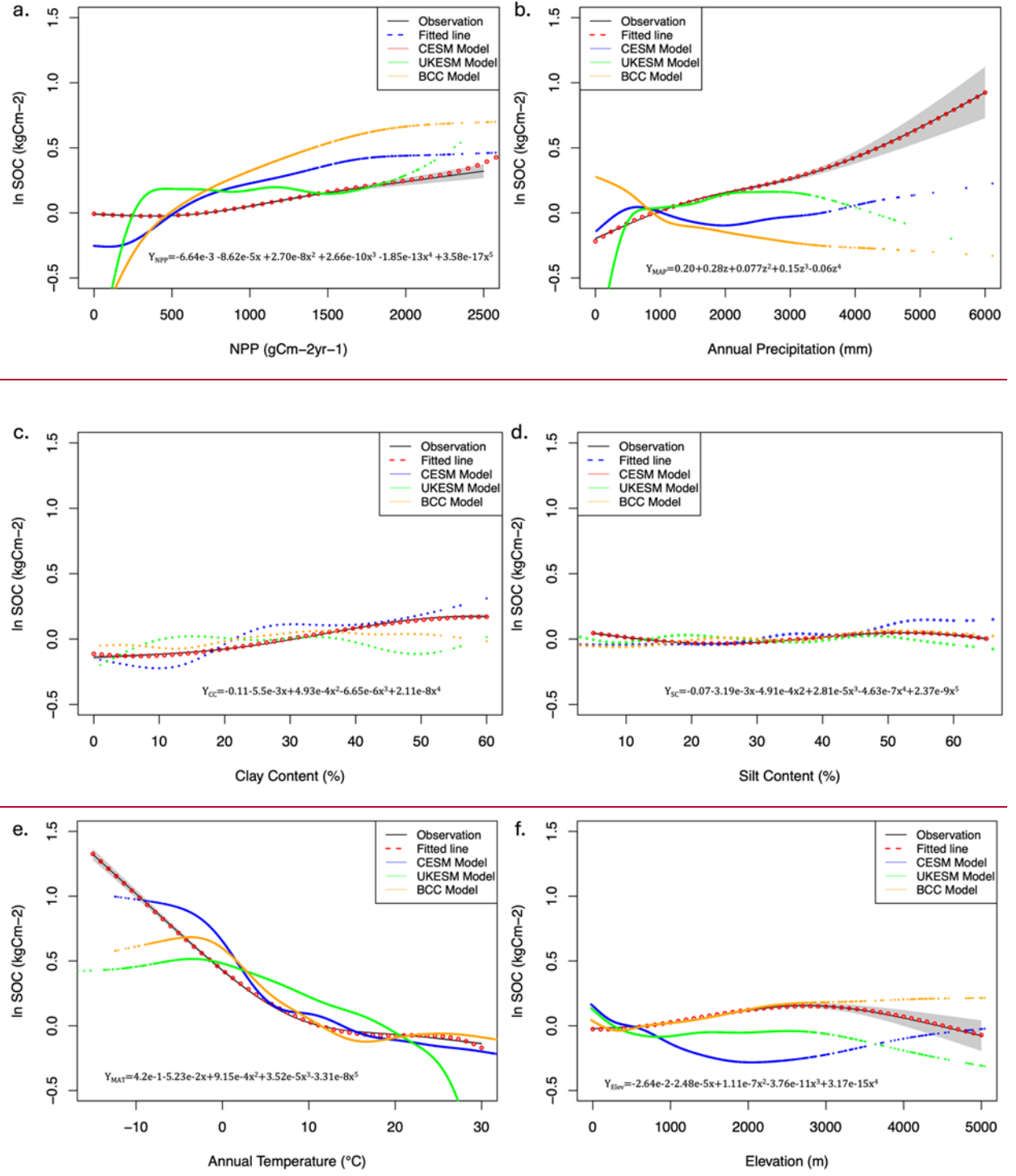


Figure 6: Predictive relationships between environmental factors and soil organic carbon stocks in observations (black line) and CMIP6 earth system models (different colors). Red circles are computed from fitted curves. The shade around the solid line indicates 95% confidence interval.

Table 1: Descriptive statistics of global soil organic carbon stocks at 0-100 cm depth interval.

Location	Minimum (kgC m ⁻²)	Maximum (kgC m ⁻²)	Mean (kgC m ⁻²)	Median (kgC m ⁻²)	Standard Deviation (kgC m ⁻²)
Global	0.14	435.30	13.50	9.50	18.20
TS broadleaf forest	0.19	314.40	10.89	8.10	14.02
Temperate broadleaf and mixed forest	0.47	312.14	16.20	12.39	17.28
Temperate grassland	0.56	315.85	12.1	8.65	16.78
Boreal forest	0.16	311.80	23.50	14.18	33.55
Cropland	0.14	435.29	12.75	9.54	16.00
Shrubland	0.19	312.54	13.59	7.59	25.63
Tundra	0.30	106.86	10.34	6.06	14.81
TS grasslands and savannas	0.32	309.13	12.60	9.16	15.17

T/S is tropical subtropical.

Table 2: Prediction accuracies of Random Forest models across biomes and at global scale in predicting SOC stocks.

Biomes	R square (Random forest)	RMSE (kgC m^{-2})
Global	0.61	0.46
TS broadleaf forest	0.54	0.46
Temperate broadleaf and mixed forest	0.50	0.53
Boreal forest	0.43	0.69
Shrubland	0.58	0.61
Cropland	0.62	0.53
Temperate grassland	0.56	0.48
Tundra	0.69	0.54
TS grasslands and savannas	0.47	0.53

T/S is tropical subtropical; RMSE is root mean square error.